ASER with QAM techniques for SISO communication system over Fisher-Snedecor *F* fading channels

Abstract: The average symbol error rate (ASER) applying various quadrature amplitude modulation (QAM) techniques is analyzed for single input and single output (SISO) system. QAM schemes are more useful to increase bandwidth efficiency for 5G and beyond wireless transmission systems. The channel of the system is influenced by Fisher-Snedecor *F* composite distribution. This distribution is commonly used to model fading channels due to its high accuracy and mathematical conformity. Various QAM schemes like hexagonal QAM, cross-QAM, square QAM and rectangular QAM are employed for ASER derivations. ASER expressions are acquired with regard to the Fox *H*-function which is the most general function and Prony approximation for Gaussian *Q*-function is utilized. Computer simulation is achieved to verify the certainty of the analyzed ASER equations.

Keywords: Fisher-Snedecor *F* fading, ASER, Quadrature amplitude modulation (QAM), Prony approximation.

1. Introduction

To enhance the bandwidth efficiency for beyond fifth-generation (B5G) cellular broadcasting systems, quadrature amplitude modulation (QAM) is a prominent technique. Concerning high-rate data communication purposes, different types of QAM methods can be employed. The hexagonal lattice-positioned signals mostly mentioned like hexagonal QAM (HQAM) is a good solution for its 2-dimensional constellations having the advantage of the most favorable Euclidean distance including comparatively poor peak-to-average power ratio (PAPR). Although HQAM gets higher-order constellations, it is a highly energy-efficient method than square QAM (SQAM). The PAPR of HQAM is lower than SQAM [1]. In the case of HQAM constellation, the symbols are located on the center of an equilateral hexagon. The applications of HQAM are found in advanced channel coding, multiple-antenna systems, optical communications, and multicarrier systems [2]. Cross-QAM (XQAM) obtains a cross shape constellation by deleting the outside edge points from rectangular QAM (RQAM) constellation, thereby reducing the peak as well as the average energy of the signal, and is appropriate for transmitting the odd count of bits per symbol. XQAM is further applied in very high-speed digital subscribers line (VDSL), asymmetric digital subscribers line (ADSL) as well as digital video broadcasting-cable (DVB-C) transmission for multimedia services [3]. The energy-efficient two-dimensional (2D) structure of XQAM is more suitable than SQAM and the odd power of 2 constellations RQAM. RQAM is a common modulation technique that covers SQAM, orthogonal binary frequency-shift keying, binary phase-shift keying (BPSK), multilevel amplitude-shift keying (ASK), quadrature phase shift keying (QPSK) modulation techniques as explicit cases [4], [5].

The typical system of the transmission is the single-input and single-output (SISO), where the transmitter uses an antenna and a single receiving antenna is employed at the receiver. The benefit of utilizing a SISO method is that it is low-cost as well as very simple to model and realize.

The channel of the system is modelled by Fisher-Snedecor *F* fading distribution. This distribution is appropriate to model the combined response of shadowing and multipath fading in the interest of recent wireless broadcasting systems. The Fisher-Snedecor *F* distribution is a common fading model of conventional fading distributions for instance Nakagami- *m*, one-sided Gaussian, and Rayleigh distribution [6] [7]. The Fisher-Snedecor *F* fading shows the most appropriate for experimental data of channel measurements like device-to-device (D2D) communications and wearable communication networks, notably at 5.8 GHz to compete with generalized-K fading in the presence of both line-of-sight (LOS) as well as non-LOS environments [7].

Recently, several research articles have analyzed ASER of QAM schemes considering fading environments. In [8], the expressions for the average symbol error probability (SEP) of the *M*-ary XQAM technique accompanying maximal-ratio combining (MRC) receiver over independent and non-identically distributed (i.n.i.d) η-μ fading channels are investigated. In the article [9], the ASER of XQAM as well as RQAM signals subject to TWDP fading channels have been analyzed with regard to Appell's as well as Laureicella's hypergeometric functions. The HQAM is found to be a very useful modulation method for energy efficiency and high data rates of beyond 5G as well as 6G wireless broadcasting strategies. The authors in [10] propose an expression for the SEP of the HQAM technique. In [11], mathematical equations of ASER for general-order RQAM, HQAM as well as 32-XQAM techniques are presented for amplify-and-forward relaying networks under i.n.i.d Nakagami-*m* fading channels. In [12], utilizations of various QAM constellations in wireless transmission are presented. In [13], the SEP of HQAM as well as RQAM for a dual-input selection combining (SC) receiver subject to η-μ fading channels is investigated for B5G. In [14], the expression for the SER of general order *M*-ary QAM is derived under the influence of the Fisher-Snedecor *F* fading channel model.

Motivated by the usefulness as well as significance, the objective of the work is to perform a mathematical investigation for the behaviour of SISO transmission scenario in the presence of Fisher-Snedecor *F* fading distribution operating with different QAM techniques. The contributions of this work are mentioned below.

● A novel SNR PDF derivation at the receiver of the SISO wireless transmission is presented with regard to Fox *H*-function.

● The useful mathematical derivations of ASER for HQAM, XQAM, RQAM and SQAM are acquired relating to Fox *H*-function, and outcomes are explained.

● The relative analysis of different QAM constellations are illustrated that reflects the superiority of XQAM over alternative QAM constellations in the SISO broadcasting system subject to Fisher-Snedecor *F* fading channels.

2. Channel model

A SISO network subject to Fisher-Snedecor *F* fading conditions is investigated. Different QAM schemes are deployed in the system. The RV L is the fading envelope, which observes the Fisher-Snedecor *F* distribution. The PDF of L is given by [7],

$$f_L(l) = \frac{2(s\Omega)^s m^m l^{2m-1}}{(ml^2 + s\Omega)^{m+s} B(m,s)} \quad . \tag{1}$$

Whereby, mean power $\Omega = E\left[l^2\right]$, m is the fading severity parameter. *s* denotes the amount of shadowing whereby $s \to \infty$ for no shadowing and $s \to 0$ for heavy shadowing, $B(.,.)$ is the beta function. Allowing $\gamma = \bar{\gamma}\frac{L^2}{\Omega}$ such that $\bar{\gamma} = E[\gamma]$ and from (1), the PDF of the instantaneous received SNR γ is described as [7]

$$f_\gamma(\gamma) = \frac{\left(s\bar{\gamma}\right)^s m^m \gamma^{m-1}}{\left(m\gamma + s\bar{\gamma}\right)^{m+h} B(m,s)}. \tag{2}$$

With the help of [15, (8.4.2.5)] and thereafter using [15, (8.3.2.21)], the expression of (2) becomes

$$f_\gamma(\gamma) = \frac{\gamma^{m-1} m^m}{B(m,s)\Gamma(m+s)\left(s\bar{\gamma}\right)^m} H_{1,1}^{1,1}\left[\frac{m\gamma}{s\bar{\gamma}}\middle|\begin{matrix}(1-m-s,1)\\(0,1)\end{matrix}\right]. \tag{3}$$

Whereby, $\Gamma(.)$ and $H_{.,.}^{.,.}[.|.]$ denote the Gamma function and Fox *H*-function respectively. Refining the Beta function, the PDF of RV γ can be expressed as

$$f_\gamma(\gamma) = \frac{\gamma^{m-1} m^m}{\Gamma(s)\Gamma(m)\left(s\bar{\gamma}\right)^m} H_{1,1}^{1,1}\left[\frac{m\gamma}{s\bar{\gamma}}\middle|\begin{matrix}(1-m-s,1)\\(0,1)\end{matrix}\right]. \tag{4}$$

3. ASER investigation

The ASER is commonly described as [16],

$$P_{ar} = \int_0^\infty p(e|\gamma) f_\gamma(\gamma) d\gamma. \tag{5}$$

Whereby, $p(e|\gamma)$ is conditional error probability which depends on the modulation technique used.

3.1 ASER analysis with HQAM over Fisher-Snedecor *F* fading channels

For *M*-ary HQAM, the CEP is written as [2] [17],

$$\Pr_{HQAM}(e|\gamma) = Y_{XX} Q\left(\sqrt{\phi\gamma}\right) + \frac{2}{3} Y_{XX} Q^2\left(\sqrt{\frac{2\phi\gamma}{3}}\right) - 2Y_{ZXX} Q\left(\sqrt{\phi\gamma}\right) Q\left(\sqrt{\frac{\phi\gamma}{3}}\right), \tag{6}$$

where, $\phi = \frac{24}{7M-4}$, $Y_{XX} = 2\left(3 - \frac{4}{\sqrt{M}} + \frac{1}{M}\right)$, as well as $Y_{ZXX} = 6\left(1 - \frac{1}{\sqrt{M}}\right)^2$. Prony approximation is the accurate approximation of the Gaussian *Q*-function $Q(.)$. Prony approximation for the Gaussian *Q*-

function with two exponential terms can be written as $Q(\tau)\approx \alpha e^{-\beta\tau^2}+\varepsilon e^{-\delta\tau^2}$ [18]. The value of the constants are $\alpha=0.208$, $\varepsilon=0.147$, $\beta=0.971$, and $\delta=0.525$. Inserting Prony approximation in (6) produces,

$$\Pr_{HQAM}(e|\gamma)=Y_{XX}\left(\alpha e^{-\beta\phi\gamma}+\varepsilon e^{-\delta\phi\gamma}\right)+\frac{2}{3}Y_{XX}\left(\alpha^2 e^{-\frac{4\beta\phi\gamma}{3}}+2\alpha\varepsilon e^{-\frac{2\beta\phi\gamma}{3}-\frac{2\delta\phi\gamma}{3}}+\varepsilon^2 e^{-\frac{4\delta\phi\gamma}{3}}\right)$$

$$-2Y_{ZXX}\left(\alpha e^{-\beta\phi\gamma}+\varepsilon e^{-\delta\phi\gamma}\right)\left(\alpha e^{-\beta\frac{\phi\gamma}{3}}+\varepsilon e^{-\delta\frac{\phi\gamma}{3}}\right). \tag{7}$$

Pretending (4) and (7) into (5), the ASER can be obtained as

$$P_{ar,HQAM}=G_1+G_2-G_3, \tag{8}$$

where,

$$G_1=Y_{XX}\Lambda\int_0^\infty\left(\alpha e^{-\beta\phi\gamma}+\varepsilon e^{-\delta\phi\gamma}\right)\gamma^{m-1}H_{1,1}^{1,1}\left[\frac{m\gamma}{s\bar{\gamma}}\middle|\begin{matrix}(1-m-s,1)\\(0,1)\end{matrix}\right]d\gamma. \tag{9}$$

$$G_2=\frac{2}{3}Y_{XX}\Lambda\int_0^\infty\left(\alpha^2 e^{-\frac{4\beta\phi\gamma}{3}}+2\alpha\varepsilon e^{-\frac{2\beta\phi\gamma}{3}-\frac{2\delta\phi\gamma}{3}}+\varepsilon^2 e^{-\frac{4\delta\phi\gamma}{3}}\right)\gamma^{m-1}H_{1,1}^{1,1}\left[\frac{m\gamma}{s\bar{\gamma}}\middle|\begin{matrix}(1-m-s,1)\\(0,1)\end{matrix}\right]d\gamma\ . \tag{10}$$

And,

$$G_3=2Y_{ZXX}\Lambda$$

$$\times\int_0^\infty\left\{\alpha^2 e^{-\gamma\left(\frac{4\beta\phi}{3}\right)}+\alpha\varepsilon e^{-\gamma\left(\beta\phi+\delta\frac{\phi}{3}\right)}+\alpha\varepsilon e^{-\gamma\left(\delta\phi+\beta\frac{\phi}{3}\right)}+\varepsilon^2 e^{-\gamma\left(\frac{4\delta\phi}{3}\right)}\right\}\gamma^{m-1}H_{1,1}^{1,1}\left[\frac{m\gamma}{s\bar{\gamma}}\middle|\begin{matrix}(1-m-s,1)\\(0,1)\end{matrix}\right]d\gamma. \tag{11}$$

Where, $\Lambda=\frac{m^m}{\Gamma(m)\Gamma(s)\left(s\bar{\gamma}\right)^m}$. Writing $e^{-\omega}=H_{0,1}^{1,0}\left[\omega\middle|\begin{matrix}-\\(0,1)\end{matrix}\right]$ from [15] and solving the integration using [15, (2.25.1.1)],

$$G_1=Y_{XX}\alpha\Lambda\left(\frac{1}{\beta\phi}\right)^m H_{2,1}^{1,2}\left[\frac{m}{\beta\phi s\bar{\gamma}}\middle|\begin{matrix}(1-m-s,1),(1-m,1)\\(0,1)\end{matrix}\right]$$

$$+Y_{XX}\varepsilon\Lambda\left(\frac{1}{\delta\phi}\right)^m H_{2,1}^{1,2}\left[\frac{m}{\delta\phi s\bar{\gamma}}\middle|\begin{matrix}(1-m-s,1),(1-m,1)\\(0,1)\end{matrix}\right], \tag{12}$$

$$G_2 = \frac{2}{3} Y_{XX} \alpha^2 \Lambda \left(\frac{3}{4\beta\phi} \right)^m H_{2,1}^{1,2} \left[\frac{3m}{4\beta\phi s \bar{\gamma}} \middle| \begin{matrix} (1-m-s,1),(1-m,1) \\ (0,1) \end{matrix} \right]$$

$$+ \frac{4}{3} Y_{XX} \alpha\varepsilon \Lambda \left(\frac{3}{2\phi(\beta+\delta)} \right)^m H_{2,1}^{1,2} \left[\frac{3m}{2(\beta+\delta)\phi s \bar{\gamma}} \middle| \begin{matrix} (1-m-s,1),(1-m,1) \\ (0,1) \end{matrix} \right]$$

$$+ \frac{2}{3} Y_{XX} \varepsilon^2 \Lambda \left(\frac{3}{4\delta\phi} \right)^m H_{2,1}^{1,2} \left[\frac{3m}{4\delta\phi s \bar{\gamma}} \middle| \begin{matrix} (1-m-s,1),(1-m,1) \\ (0,1) \end{matrix} \right]. \tag{13}$$

And,

$$G_3 = 2 Y_{ZXX} \alpha^2 \Lambda \left(\frac{3}{4\beta\phi} \right)^m H_{2,1}^{1,2} \left[\frac{3m}{4\beta\phi s \bar{\gamma}} \middle| \begin{matrix} (1-m-s,1),(1-m,1) \\ (0,1) \end{matrix} \right]$$

$$+ 2 Y_{ZXX} \alpha\varepsilon \Lambda \left(\frac{3}{(3\beta+\delta)\phi} \right)^m H_{2,1}^{1,2} \left[\frac{3m}{(3\beta+\delta)\phi s \bar{\gamma}} \middle| \begin{matrix} (1-m-s,1),(1-m,1) \\ (0,1) \end{matrix} \right]$$

$$+ 2 Y_{ZXX} \alpha\varepsilon \Lambda \left(\frac{3}{(3\delta+\beta)\phi} \right)^m H_{2,1}^{1,2} \left[\frac{3m}{(3\delta+\beta)\phi s \bar{\gamma}} \middle| \begin{matrix} (1-m-s,1),(1-m,1) \\ (0,1) \end{matrix} \right]$$

$$+ 2 Y_{ZXX} \varepsilon^2 \Lambda \left(\frac{3}{4\delta\phi} \right)^m H_{2,1}^{1,2} \left[\frac{3m}{4\delta\phi s \bar{\gamma}} \middle| \begin{matrix} (1-m-s,1),(1-m,1) \\ (0,1) \end{matrix} \right]. \tag{14}$$

3.2 ASER analysis with XQAM over Fisher-Snedecor *F* fading channels

For $L \times M$ XQAM, the $\Pr(e|\gamma)$ is written as [19],

$$\Pr_{XQAM}(e|\gamma) = A_{XX} Q\left(\zeta\sqrt{\gamma}\right) - A_{ZXX} Q^2\left(\zeta\sqrt{\gamma}\right). \tag{15}$$

Whereby $\zeta = \sqrt{\frac{96}{31L \times M - 32}}$, $A_{XX} = 2\left(2 - \frac{1}{L} - \frac{1}{M}\right)$, and $A_{ZXX} = 4\left(1 - \frac{1}{L} - \frac{1}{M} + \frac{2}{L+M}\right)$. Putting the Prony approximation in (15), $\Pr(e|\gamma)$ is rephrased as

$$\Pr_{XQAM}(e|\gamma) = A_{XX}\left(\alpha e^{-\beta\zeta^2\gamma} + \varepsilon e^{-\delta\zeta^2\gamma}\right) - A_{ZXX}\left(\alpha^2 e^{-2\beta\zeta^2\gamma} + \varepsilon^2 e^{-2\delta\zeta^2\gamma} + 2\alpha\varepsilon e^{-\beta\zeta^2\gamma-\delta\zeta^2\gamma}\right). \tag{16}$$

Inserting (16) and (4) into (5), the ASER can be written as

$$P_{ar,XQAM} = I_1 - I_2. \tag{17}$$

Whereby,

$$I_1 = A_{XX}\Lambda\int_0^\infty \left(\alpha e^{-\beta\zeta^2\gamma} + \varepsilon e^{-\delta\zeta^2\gamma}\right)\gamma^{m-1} H_{1,1}^{1,1}\left[\frac{m\gamma}{s\bar{\gamma}}\middle| \begin{matrix}(1-m-s,1)\\(0,1)\end{matrix}\right] d\gamma . \tag{18}$$

And,

$$I_2 = A_{ZXX}\Lambda\int_0^\infty \left(\alpha^2 e^{-2\beta\zeta^2\gamma} + 2\alpha\varepsilon e^{-\beta\zeta^2\gamma-\delta\zeta^2\gamma} + \varepsilon^2 e^{-2\delta\zeta^2\gamma}\right)\gamma^{m-1} H_{1,1}^{1,1}\left[\frac{m\gamma}{s\bar{\gamma}}\middle| \begin{matrix}(1-m-s,1)\\(0,1)\end{matrix}\right] d\gamma . \tag{19}$$

Replacing the exponential terms with Fox *H*-function and solving the integration using [15, (2.25.1.1)],

$$I_1 = \frac{A_{XX}\alpha\Lambda}{\left(\beta\zeta^2\right)^m} H_{2,1}^{1,2}\left[\frac{m}{\beta\zeta^2 s\bar{\gamma}}\middle| \begin{matrix}(1-m-s,1),(1-m,1)\\(0,1)\end{matrix}\right]$$

$$+\frac{A_{XX}\varepsilon\Lambda}{\left(\delta\zeta^2\right)^m} H_{2,1}^{1,2}\left[\frac{m}{\delta\zeta^2 s\bar{\gamma}}\middle| \begin{matrix}(1-m-s,1),(1-m,1)\\(0,1)\end{matrix}\right] . \tag{20}$$

And,

$$I_2 = \frac{A_{ZXX}\alpha^2\Lambda}{\left(2\beta\zeta^2\right)^m} H_{2,1}^{1,2}\left[\frac{m}{2\beta\zeta^2 s\bar{\gamma}}\middle| \begin{matrix}(1-m-s,1),(1-m,1)\\(0,1)\end{matrix}\right]$$

$$+\frac{2A_{ZXX}\alpha\varepsilon\Lambda}{\left\{(\beta+\delta)\zeta^2\right\}^m} H_{2,1}^{1,2}\left[\frac{m}{(\beta+\delta)\zeta^2 s\bar{\gamma}}\middle| \begin{matrix}(1-m-s,1),(1-m,1)\\(0,1)\end{matrix}\right]$$

$$+\frac{A_{ZXX}\varepsilon^2\Lambda}{\left(2\delta\zeta^2\right)^m} H_{2,1}^{1,2}\left[\frac{m}{2\delta\zeta^2 s\bar{\gamma}}\middle| \begin{matrix}(1-m-s,1),(1-m,1)\\(0,1)\end{matrix}\right] . \tag{21}$$

3.3 ASER analysis with SQAM over Fisher-Snedecor *F* fading channels

For *M*-ary SQAM, the $\Pr\left(e|\gamma\right)$ can be expressed as [19],

$$\Pr_{SQAM}\left(e|\gamma\right) = B_{XX} Q\left(\mu\sqrt{\gamma}\right) - B_{ZXX} Q^2\left(\mu\sqrt{\gamma}\right). \tag{22}$$

Where $\mu = \sqrt{\frac{3}{M-1}}$, $B_{XX} = 4\left(1-\frac{1}{\sqrt{M}}\right)$, and $B_{ZXX} = 4\left(1-\frac{1}{\sqrt{M}}\right)^2$. Replacing $Q(.)$ with the Prony approximation,

$$\Pr_{SQAM}\left(e|\gamma\right) = B_{XX}\left(\alpha e^{-\beta\mu^2\gamma} + \varepsilon e^{-\delta\mu^2\gamma}\right) - B_{ZXX}\left(\alpha^2 e^{-2\beta\mu^2\gamma} + \varepsilon^2 e^{-2\delta\mu^2\gamma} + 2\alpha\varepsilon e^{-\beta\mu^2\gamma-\delta\mu^2\gamma}\right). \tag{23}$$

Substituting (23) and (4) into (5), the ASER can be obtained as

$$P_{ar,SQAM} = J_1 - J_2 \ . \tag{24}$$

Where,

$$J_1 = B_{XX}\Lambda\int_0^\infty \left(\alpha e^{-\beta\mu^2\gamma} + \varepsilon e^{-\delta\mu^2\gamma}\right)\gamma^{m-1} H_{1,1}^{1,1}\left[\frac{m\gamma}{s\bar{\gamma}}\middle|\begin{matrix}(1-m-s,1)\\(0,1)\end{matrix}\right]d\gamma \ , \tag{25}$$

and,

$$J_2 = B_{ZXX}\Lambda\int_0^\infty \left(\alpha^2 e^{-2\beta\mu^2\gamma} + 2\alpha\varepsilon e^{-\beta\mu^2\gamma-\delta\mu^2\gamma} + \varepsilon^2 e^{-2\delta\mu^2\gamma}\right)\gamma^{m-1} H_{1,1}^{1,1}\left[\frac{m\gamma}{s\bar{\gamma}}\middle|\begin{matrix}(1-m-s,1)\\(0,1)\end{matrix}\right]d\gamma \ . \tag{26}$$

Expressing the exponential terms with Fox *H*-function and solving the integrals with the help of [15, (2.25.1.1)],

$$J_1 = \frac{B_{XX}\alpha\Lambda}{\left(\beta\mu^2\right)^m} H_{2,1}^{1,2}\left[\frac{m}{\beta\mu^2 s\bar{\gamma}}\middle|\begin{matrix}(1-m-s,1),(1-m,1)\\(0,1)\end{matrix}\right]$$
$$+\frac{B_{XX}\varepsilon\Lambda}{\left(\delta\mu^2\right)^m} H_{2,1}^{1,2}\left[\frac{m}{\delta\mu^2 s\bar{\gamma}}\middle|\begin{matrix}(1-m-s,1),(1-m,1)\\(0,1)\end{matrix}\right], \tag{27}$$

and

$$J_2 = \frac{B_{ZXX}\alpha^2\Lambda}{\left(2\beta\mu^2\right)^m} H_{2,1}^{1,2}\left[\frac{m}{2\beta\mu^2 s\bar{\gamma}}\middle|\begin{matrix}(1-m-s,1),(1-m,1)\\(0,1)\end{matrix}\right]$$
$$+\frac{2B_{ZXX}\alpha\varepsilon\Lambda}{\left\{\left(\beta+\delta\right)\mu^2\right\}^m} H_{2,1}^{1,2}\left[\frac{m}{\left(\beta+\delta\right)\mu^2 s\bar{\gamma}}\middle|\begin{matrix}(1-m-s,1),(1-m,1)\\(0,1)\end{matrix}\right]$$
$$+\frac{B_{ZXX}\varepsilon^2\Lambda}{\left(2\delta\mu^2\right)^m} H_{2,1}^{1,2}\left[\frac{m}{2\delta\mu^2 s\bar{\gamma}}\middle|\begin{matrix}(1-m-s,1),(1-m,1)\\(0,1)\end{matrix}\right]. \tag{28}$$

3.4 ASER analysis for RQAM under Fisher-Snedecor *F* fading channels

For $L \times M$ RQAM, the $\Pr\left(e|\gamma\right)$ can be given as [20],

$$\Pr_{RQAM}\left(e|\gamma\right) = C_{XX}Q\left(q\sqrt{\gamma}\right) + C_{ZXX}Q\left(r\sqrt{\gamma}\right) - C_{XX}C_{ZXX}Q\left(q\sqrt{\gamma}\right)Q\left(r\sqrt{\gamma}\right). \tag{29}$$

Where, $C_{XX} = 2\left(1-\frac{1}{L}\right)$; $C_{ZXX} = 2\left(1-\frac{1}{M}\right)$; $q = \sqrt{\frac{6}{\left(L^2-1\right)+\left(M^2-1\right)b^2}}$; $r = bq$; $b = d_Q / d_I$ Here d_I and d_Q are in-phase as well as quadrature decision distance, respectively. Again applying the Prony approximation in (29), $\Pr\left(e|\gamma\right)$ is arranged as

$$\Pr_{RQAM}\left(e|\gamma\right) = C_{XX}\left(\alpha e^{-\beta q^2\gamma} + \varepsilon e^{-\delta q^2\gamma}\right) + C_{ZXX}\left(\alpha e^{-\beta r^2\gamma} + \varepsilon e^{-\delta r^2\gamma}\right)$$
$$-C_{XX}C_{ZXX}\left(\alpha^2 e^{-\beta q^2\gamma-\beta r^2\gamma} + \alpha\varepsilon e^{-\beta q^2\gamma-\delta r^2\gamma} + \alpha\varepsilon e^{-\delta q^2\gamma-\beta r^2\gamma} + \varepsilon^2 e^{-\delta q^2\gamma-\delta r^2\gamma}\right). \tag{30}$$

Putting (30) and (4) into (5), the ASER can be obtained as

$$P_{ar,RQAM} = K_1 + K_2 - K_3 \ . \tag{31}$$

Where,

$$K_1 = C_{XX}\Lambda\int_0^\infty\left(\alpha e^{-\beta q^2\gamma} + \varepsilon e^{-\delta q^2\gamma}\right)\gamma^{m-1}H_{1,1}^{1,1}\left[\frac{m\gamma}{s\bar{\gamma}}\middle|\begin{matrix}(1-m-s,1)\\(0,1)\end{matrix}\right]d\gamma\ , \tag{32}$$

$$K_2 = C_{ZXX}\Lambda\int_0^\infty\left(\alpha e^{-\beta r^2\gamma} + \varepsilon e^{-\delta r^2\gamma}\right)\gamma^{m-1}H_{1,1}^{1,1}\left[\frac{m\gamma}{s\bar{\gamma}}\middle|\begin{matrix}(1-m-s,1)\\(0,1)\end{matrix}\right]d\gamma\ , \tag{33}$$

And

$$K_3 = C_{XX}C_{ZXX}\Lambda$$
$$\times\int_0^\infty\left(\alpha^2 e^{-\beta q^2\gamma-\beta r^2\gamma} + \alpha\varepsilon e^{-\beta q^2\gamma-\delta r^2\gamma} + \alpha\varepsilon e^{-\delta q^2\gamma-\beta r^2\gamma} + \varepsilon^2 e^{-\delta q^2\gamma-\delta r^2\gamma}\right)\gamma^{m-1}H_{1,1}^{1,1}\left[\frac{m\gamma}{s\bar{\gamma}}\middle|\begin{matrix}(1-m-s,1)\\(0,1)\end{matrix}\right]d\gamma\ . \tag{34}$$

Writing the exponential terms with Fox *H*-function and simplifying the integrals by means of [15, (2.25.1.1)],

$$K_1 = \frac{C_{XX}\alpha\Lambda}{\left(\beta q^2\right)^m}H_{2,1}^{1,2}\left[\frac{m}{\beta q^2 s\bar{\gamma}}\middle|\begin{matrix}(1-m-s,1),(1-m,1)\\(0,1)\end{matrix}\right]$$
$$+\frac{C_{XX}\varepsilon\Lambda}{\left(\delta q^2\right)^m}H_{2,1}^{1,2}\left[\frac{m}{\delta q^2 s\bar{\gamma}}\middle|\begin{matrix}(1-m-s,1),(1-m,1)\\(0,1)\end{matrix}\right], \tag{35}$$

$$K_2 = \frac{C_{ZXX}\alpha\Lambda}{\left(\beta r^2\right)^m}H_{2,1}^{1,2}\left[\frac{m}{\beta r^2 s\bar{\gamma}}\middle|\begin{matrix}(1-m-s,1),(1-m,1)\\(0,1)\end{matrix}\right]$$

$$+\frac{C_{ZXX}\varepsilon\Lambda}{\left(\delta r^2\right)^m}H_{2,1}^{1,2}\left[\frac{m}{\delta r^2 s\bar{\gamma}}\left|\begin{matrix}(1-m-s,1),(1-m,1)\\(0,1)\end{matrix}\right.\right], \tag{36}$$

and

$$K_3=\frac{C_{XX}C_{ZXX}\alpha^2\Lambda}{\left\{\left(q^2+r^2\right)\beta\right\}^m}H_{2,1}^{1,2}\left[\frac{m}{\left(q^2+r^2\right)\beta s\bar{\gamma}}\left|\begin{matrix}(1-m-s,1),(1-m,1)\\(0,1)\end{matrix}\right.\right]$$

$$+\frac{C_{XX}C_{ZXX}\alpha\varepsilon\Lambda}{\left(\beta q^2+\delta r^2\right)^m}H_{2,1}^{1,2}\left[\frac{m}{\left(\beta q^2+\delta r^2\right)s\bar{\gamma}}\left|\begin{matrix}(1-m-s,1),(1-m,1)\\(0,1)\end{matrix}\right.\right]$$

$$+\frac{C_{XX}C_{ZXX}\alpha\varepsilon\Lambda}{\left(\delta q^2+\beta r^2\right)^m}H_{2,1}^{1,2}\left[\frac{m}{\left(\delta q^2+\beta r^2\right)s\bar{\gamma}}\left|\begin{matrix}(1-m-s,1),(1-m,1)\\(0,1)\end{matrix}\right.\right]$$

$$+\frac{C_{XX}C_{ZXX}\varepsilon^2\Lambda}{\left\{\left(q^2+r^2\right)\delta\right\}^m}H_{2,1}^{1,2}\left[\frac{m}{\left(q^2+r^2\right)\delta s\bar{\gamma}}\left|\begin{matrix}(1-m-s,1),(1-m,1)\\(0,1)\end{matrix}\right.\right]. \tag{37}$$

4. Numerical outcomes and analysis

The analytical expressions of the previous section are evaluated and illustrated here. In Figure 1, the ASER vs. average SNR curves have been presented for 16-HQAM and 32-HQAM schemes over different values of fading parameter *m* and shadowing parameter *s*. It can be realized that ASER performance is poor with 32-HQAM in compared to 16-HQAM, which is owing to the evidence that the limited constellation size is less affected by fading effects. The ASER performance improves with the increase in the amount of fading parameter *m*, signifying that the channel fading develops into less stringent. In addition, at high average SNR, the ASER performance enhances, along an increment in shadowing parameter *s*, referring that the channel turns into lower shadowing.

In Figure 2, ASER vs. average SNR has been analyzed for 4x4 XQAM as well as 8x4 XQAM techniques subject to different values of *m* and *s*. It is observed that ASER performance is better with 4x4 XQAM compared to 8x4 XQAM, since large constellation size is more affected by channel fading. Moreover, the ASER performance boosts with an addition of fading parameter *m*, signifying the betterment of fading situation. At a high average SNR, the ASER reduces as *s* enhances because the large value of *s* indicates the influence of minor shadowing.

In Figure 3, ASER vs. average SNR has been analyzed for 16-SQAM and 32-SQAM techniques by varying the values of *m* and *s* respectively. ASER performance becomes better with 16-SQAM as compared to 32-SQAM since the small constellation size may overcome the fading effect much better. The ASER increases while the amount of fading parameter *m* decreases for a certain constellation size. This is by reason of the lower the amount of *m*, more is the fading issue. Likewise, ASER deteriorates while the shadowing parameter *s* decrease, which is because of heavy shadowing.

In Figure 4, ASER vs. Average SNR has been illustrated for 4x4 RQAM and for 8x4 RQAM over different values of *m* and *s*. Here decision distance ratio β=1. ASER value is much less for 4x4 RQAM than 8x4 RQAM. Large constellation size suffers more fading effects. ASER performance becomes better with an increase in *m* due to less fading effect. ASER performance improves at high average SNR with an increase in *s* due to light shadowing.

In Figure 5, the ASER plots have been shown considering different QAM schemes with *m* = 2 and *s* = 0.5. ASER performance improves with XQAM as compared to RQAM since the XQAM technique has less peak as well as average signal power than RQAM.

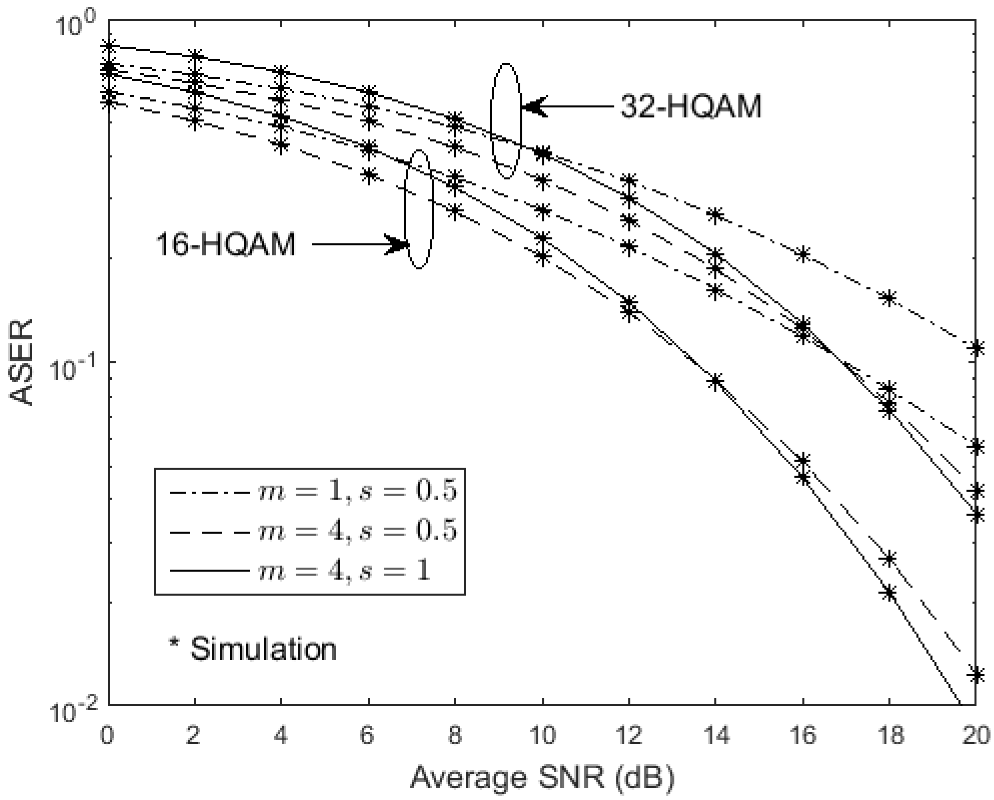

Figure 1. ASER vs. Average SNR (dB) of the explored SISO system using HQAM for different *m* and *s*.

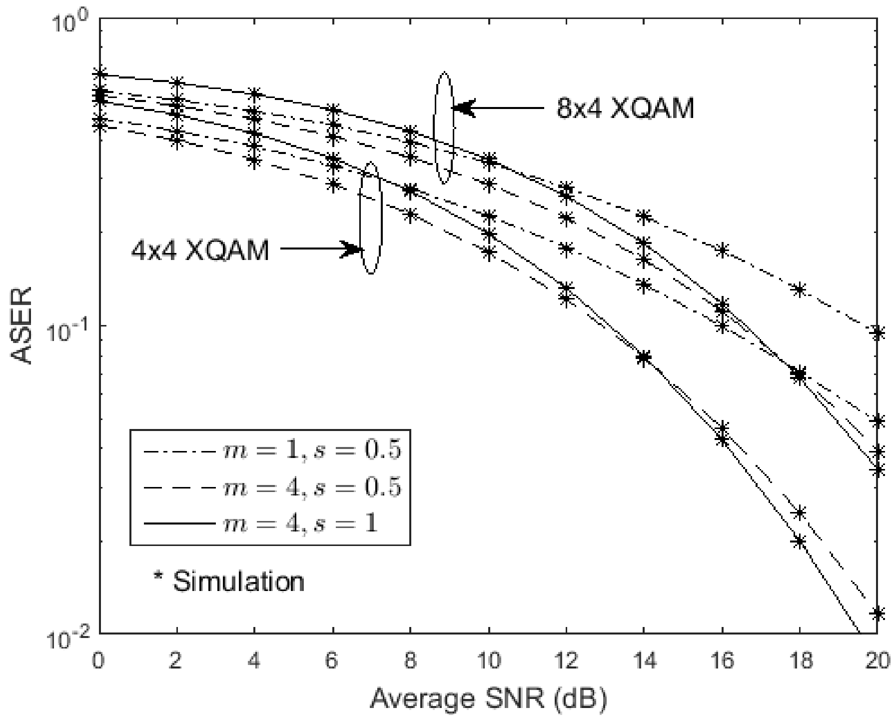

Figure 2. ASER vs. Average SNR (dB) of the investigated SISO system using XQAM for different *m* and *s*.

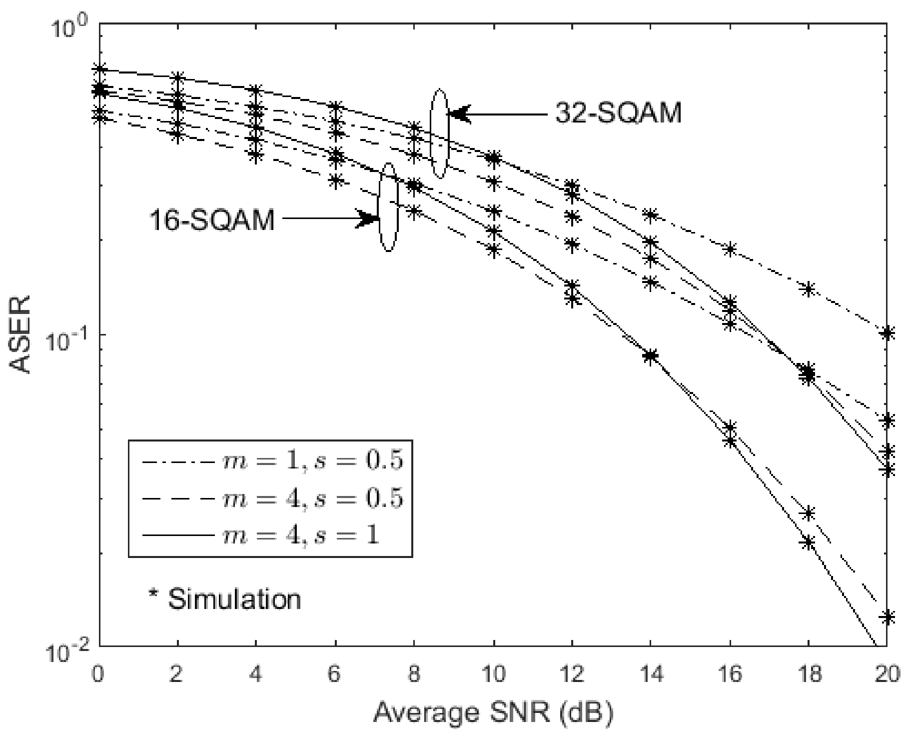

Figure 3. ASER vs. Average SNR (dB) of the examined SISO system using SQAM for different *m* and *s*.

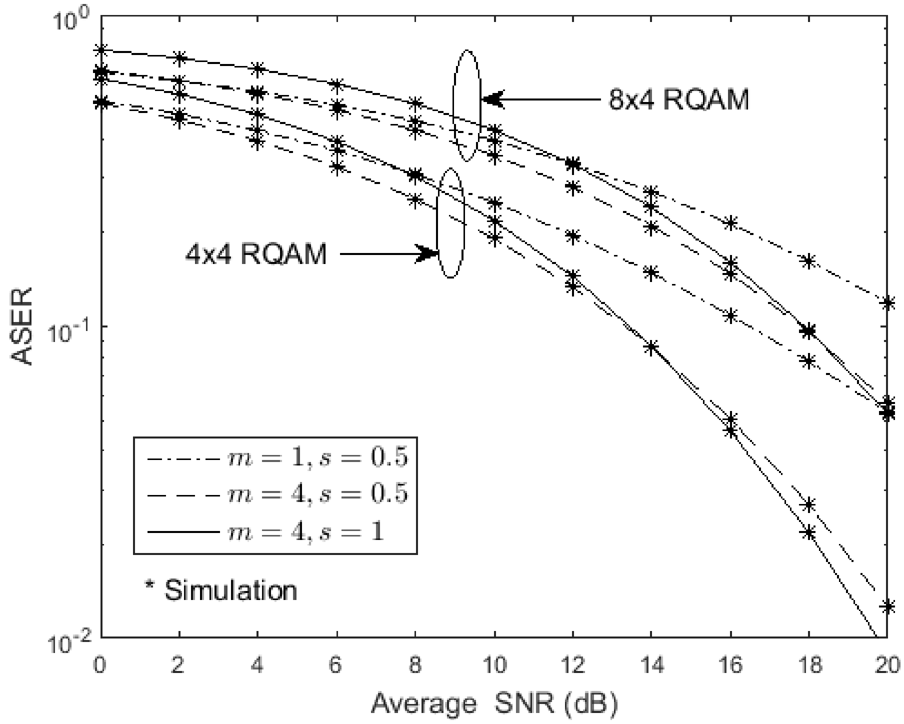

Figure 4. ASER vs. Average SNR (dB) of the observed SISO system using RQAM for different *m* and *s*.

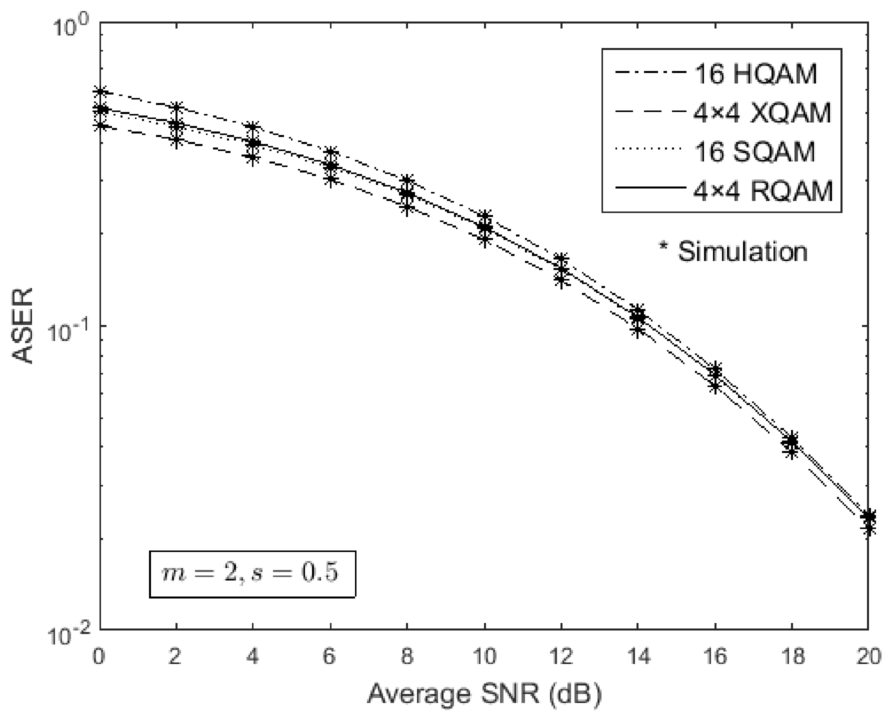

Figure 5. Comparison of ASER vs. Average SNR (dB) of the analysed SISO system utilizing different QAM techniques and for m = 2, s = 0.5.

5. Conclusions

The ASER of the SISO communication system subject to Fisher-Snedecor F fading channels is investigated in this article. Various types of QAM techniques like HQAM, XQAM, SQAM and RQAM are applied to find the ASER. The most accurate Prony approximation is utilized for Gaussian Q -function. The expressions of ASER are conferred with regard to the Fox H-function. The arbitrary value of shadowing parameter, and fading parameter are considered for the analysis. The arbitrary number of constellation sizes for different QAM techniques are utilized to illustrate the ASER. The use of the low value of constellation size gives a better ASER performance in general since the number of symbols get affected by the operating environment is less. Again when the channel is influenced by less fading i.e. for the large fading parameter the ASER performance improves and for the high value of the shadowing parameter i.e. for the light shadowing environment the ASER performance improves. Finally, computer-simulated data have been included to determine the accuracy of the derived analytical formations.

References:

[1] M. Tanahashi and H. Ochiai, "A multilevel coded modulation approach for hexagonal signal constellation," IEEE Transactions on Wireless Communications, vol. 8, no. 10, pp. 4993–4997, Oct. 2009.

[2] Luca Rugini, "Symbol error probability of hexagonal QAM," IEEE Communications Letters, vol. 20, no. 8, pp. 1523–1526, Aug. 2016.

[3] X.-C. Zhang, H. Yu, and G. Wei, "Exact symbol error probability of cross-QAM in AWGN and fading channels," EURASIP Journal on Wireless Communications and Networking, vol. 2010, pp. 1–9, Nov. 2010.

[4] D. Dixit and P. R. Sahu, "Performance analysis of rectangular QAM with SC receiver over Nakagami-*m* fading channels," IEEE Communications Letters, vol. 18, no. 7, pp. 1262–1265, Jul. 2014.

[5] J. P. Peña-Martín, J. M. Romero-Jerez, and C. Tellez-Labao, "Performance of selection combining diversity in η −μ fading channels with integer values of μ," IEEE Transactions on Vehicular Technology, vol. 64, no. 2, pp. 834–839, Feb. 2015.

[6] O. S. Badarneh, D. B. da Costa, P. C. Sofotasios, S. Muhaidat, and S. L. Cotton, "On the sum of Fisher-Snedecor F variates and its application to maximal-ratio-combining," IEEE Wireless Communications Letters, vol. 7, no. 6, pp. 966–969, December 2018. https://doi.org/10.1109/LWC.2018.2836453

[7] S. K. Yoo, S. L. Cotton, P. C. Sofotasios, M. Matthaiou, M. Valkama, and G. K. Karagiannidis, "The Fisher-Snedecor F distribution: A simple and accurate composite fading model," IEEE Communications Letters, vol. 21, no. 7, pp. 1661-1664, July 2017. https://doi.org/10.1109/LCOMM.2017.2687438

[8] Hua Yu, Gang Wei, Fei Ji, and Xichun Zhang, "On the error probability of cross-QAM with MRC reception over generalized η-μ fading channels," IEEE Transactions on Vehicular Technology, vol. 60, no. 6, pp. 2631 - 2643, July 2011. DOI: 10.1109/TVT.2011.2154347

[9] Dharmendra Dixit and P. R. Sahu, "Performance of QAM signaling over TWDP fading channels," IEEE Transactions on Wireless Communications, vol. 12, no. 4, pp. 1794-1799, April 2013.

[10] Thrassos K. Oikonomou , Sotiris A. Tegos , Dimitrios Tyrovolas , Panagiotis D. Diamantoulakis , and George K. Karagiannidis , “On the error analysis of hexagonal-QAM constellations,” IEEE Communications Letters, vol. 26, no. 8, pp. 1764-1768, August 2022.

[11] Nagendra Kumar, Praveen Kumar Singya , and Vimal Bhatia, “ASER analysis of hexagonal and rectangular QAM schemes in multiple-relay networks,” IEEE Transactions on Vehicular Technology, vol. 67, no. 2, pp. 1815-1819, February 2018.

[12] Praveen Kumar Singya, Parvez Shaik, Nagendra Kumar, Vimal Bhatia, and Mohamed-Slim Alouini, “A survey on higher-order QAM constellations: technical challenges, recent advances, and future trends,” IEEE Open Journal of the Communications Society, vol. 2, pp. 617-655, March 2021.

[13] Mehmet Bilim, “Dual-branch SC wireless systems with HQAM for beyond 5G over η-μ fading channels,” Peer-to-Peer Networking and Applications, vol.14, pp. 305–318, 2021.

[14] Taimour Aldalgamouni, Mehmet Cagri Ilter, Osamah S. Badarneh, and Halim Yanikomeroglu, “Performance analysis of Fisher-Snedecor *F* composite fading channels,” 2018 IEEE Middle East and North Africa Communications Conference (MENACOMM), Jounieh, Lebanon, April 2018.

[15] A. P. Prudnikov, Y. A. Brychkov, and O. I. Marichev, Integrals and series: more special functions, vol. 3. Gordon and Breach Science Publishers, 1990.

[16] J. G. Proakis, Digital Communications, 4th Edition, McGraw-Hill, 2001.

[17] Mehmet Bilim, “Different QAM schemes analyses for ARS fading channels,” Transactions on Emerging Telecommunications Technologies, vol. 32, no. 1, e4119, September 2020.

[18] Pavel Loskot, and Norman C. Beaulieu, “Prony and Polynomial approximations for evaluation of the average probability of error over slow-fading channels," IEEE Transactions on Vehicular Technology, vol. 58, no. 3, pp. 1269-1280, March 2009.

[19] Dharmendra Sadhwani, “Simple and tightly approximated integrals over κ-μ shadowed fading channel with applications,” IEEE Transactions On Vehicular Technology, vol. 67, no. 10, pp. 10092-10096, October 2018.

[20] N. C. Beaulieu, “A useful integral for wireless communication theory and its application to rectangular signaling constellation error rates,” IEEE Transactions on Communications, vol. 54, no. 5, pp. 802–805, May 2006. https://doi.org/10.1109/TCOMM.2006.874003